Fig. 2. In situ hybridization of *PAPST1* mRNA and immunohistochemical staining for PAPST1 and PAPST2 proteins in colorectal carcinoma. (**A** and **B**) Serial frozen sections from rectal carcinoma were hybridized with either a digoxigenin-labeled antisense (A) or sense (B) riboprobe against *PAPST1* mRNA. Hybridized probes were detected with an alkaline phosphatase-labeled anti-digoxigenin antibody. Bar scales are 50 μm. (**C** and **D**) The specificity of anti-PAPST1 antibody to human PAPST1 (hPAPST1) protein. A pCXN2-c-myc expression vector containing the *hPAPST1* gene was transfected into HEK293 cells and the cell lysate was prepared. hPAPST1 protein was detected by western blotting using anti-c-myc (C) or anti-PAPST1 (D) antibodies. Arrows indicate the band of hPAPST1 protein. None, intact cells; mock, cells treated with empty vector; myc-hPAPST1, cells treated with pCXN2-c-myc-hPAPST1. IB, immunoblot; Ab, antibody. (**E–F'**) Paraffin-embedded sections were immunostained with anti-PAPST1 antibody using an automated Ventana system. Sections were counterstained with hematoxylin. (E and E') Noncancerous colorectal tissue and (F and F') cancerous colorectal tissue. PAPST1 protein was predominantly detected as perinuclear dots in epithelial carcinoma cells (F', arrowheads). In both noncancerous (E and E') and cancerous (F and F') colorectal tissues, stromal cells were weakly stained, whereas epithelial cells were strongly stained. Representative results from 19 (E) and 20 (F) stains are shown. Bar scales are 200 μm (E and F) and 50 μm (E' and F'). (E and F), low magnification; (E' and F'), high magnification. (**G–K**) Frozen sections were immunostained with anti-PAPST1 (G–I) or anti-PAPST2 (J and K) antibody and detected with anti-rabbit IgG conjugated Alexa Flour 488 (green). F-actin filaments and nuclei were counterstained with phallotoxin-conjugated Alexa Fluor 594 (red) and with Hoechst 33342 (blue), respectively. (G, G' and J) Noncancerous colorectal tissues and (H, I and K) cancerous colorectal tissues. In both noncancerous and cancerous colorectal tissues, PAPST1 protein was detected in the perinuclear region (Golgi apparatus) of epithelial cells (G, G' and H, arrowheads) and stromal cells (G, G' and I, arrows). Fibroblasts were heavily stained with PAPST1 antibody in the vicinity of invasive cancer cells where the desmoplastic reaction was observed (I, asterisks). PAPST2 protein was strongly detected in cells of hematopoietic lineage (diamond arrows) in both noncancerous (J) and cancerous (K) colorectal tissues. Epithelial cells were stained with anti-PAPST2 antibody in noncancerous colorectal tissues (J), whereas they were only faintly stained in cancerous colorectal tissues (K). Bar scales are 50 μm. (G), low magnification; (G'), high magnification.
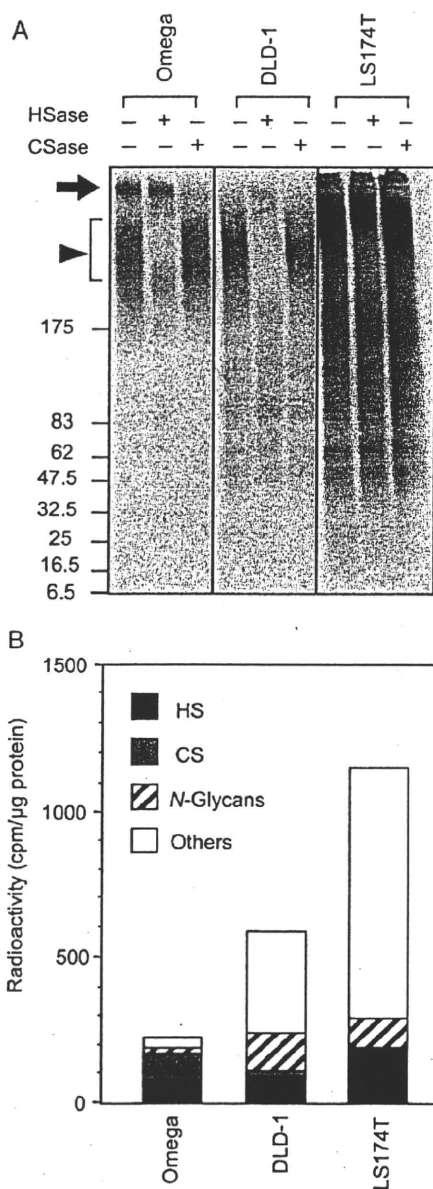
Fig. 4. Knockdown efficiency of each siRNA for *PAPST1* (left panel) and *PAPST2* (right panel) transcripts. Relative amounts of each transcript were quantified using real-time PCR and normalized with respect to the amount of *GAPDH*. Values shown are means (SDs) obtained from three independent experiments. No siRNA, cells treated with no siRNA; control (100 nM), cells treated with 100 nM control siRNA; control (200 nM), cells treated with 200 nM control siRNA; PAPST1, cells treated with 100 nM *PAPST1* siRNA; PAPST2, cells treated with 100 nM *PAPST2* siRNA; PAPST1 + PAPST2, cells treated with 100 nM *PAPST1* siRNA and 100 nM *PAPST2* siRNA.

N-glycans. LS174T contained a substantial amount of extra sulfate, which was considered to be represented by sulfated mucins and sulfated tyrosine residues of proteins.

Gene silencing of PAPS transporters reduces sulfation in DLD-1 cells

To address whether the expression status of PAPS transporters affects sulfation in colorectal carcinomas, the expression of PAPS transporter genes in a colorectal carcinoma cell line was reduced via RNA interference (RNAi). For the RNAi experiments, *PAPST1* siRNA (small interfering RNA), *PAPST2* siRNA and a control siRNA that did not match any human gene were used. On the basis of knockdown efficiency, DLD-1 was selected among the three cell lines. We decided to introduce siRNA in three separate sequential additions because a single addition was found to have a slight effect on the sulfation modification. On days 1, 4 and 7, each of these siRNAs was repeatedly transfected into DLD-1 cells, and the knockdown efficiency was determined by real-time PCR on day 10 (i.e. 3 days after the third transfection). Figure 4 shows the expression of *PAPST1* and *PAPST2* genes in DLD-1 cells treated with each siRNA. Treatment with *PAPST1* and *PAPST2* siRNAs was found to reduce the expression level of the corresponding gene to <20% of the original level. Double knockdown with *PAPST1* and *PAPST2* siRNAs reduced both transcripts in the DLD-1 cells. No significant alteration was observed in the expression level of the nontargeted gene.

Fig. 3. Metabolic labeling of colorectal carcinoma cell lines. (A) Autoradiograph of radioactivity incorporated into cellular proteins. Omega, DLD-1 and LS174T cells were labeled with Na$_2$[^{35}S]O$_4$ for 24 h and treated in the presence or absence of heparitinase (HSase) or chondroitinase ABC (CSase) for 2 h. Cellular proteins were separated by 2–15% gradient SDS–PAGE. The arrowhead and arrow indicate signals that disappear upon treatment with HSase and CSase, respectively. (B) The ratio of sulfate incorporation into HS, CS and *N*-glycans in cellular proteins. The amounts of sulfate incorporated into HS, CS and *N*-glycans were estimated on the basis of the radioactivity released after treatment of cells or cellular proteins with HSase, CSase and PNGase F, respectively. The amount of total sulfate incorporation into proteins was determined by precipitation of the proteins in the cell lysate with TCA.

other glycans. Consistent with the results of autoradiography, Omega cells were found to contain high levels of HS and CS and lower levels of sulfated *N*-glycans. DLD-1 and LS174T cells had low levels of CS but high levels of HS and
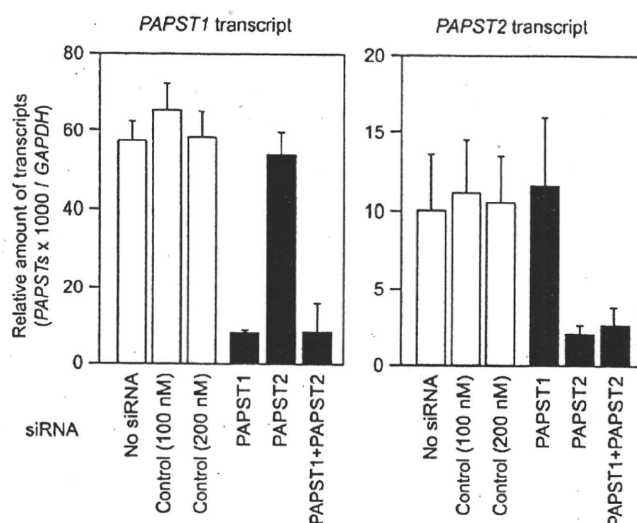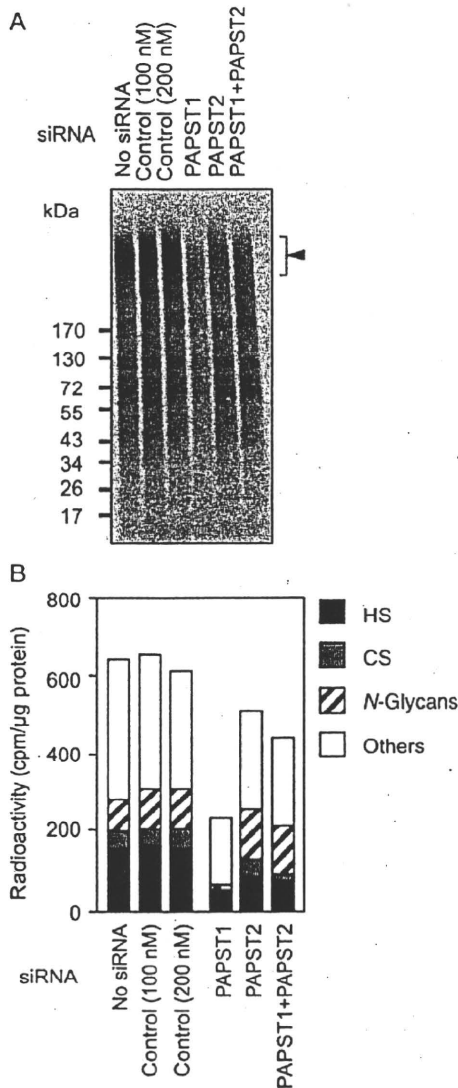
A

B

Fig. 5. Metabolic labeling of DLD-1 cells treated with siRNAs. DLD-1 cells were treated with various siRNAs on days 1, 4 and 7 and analyzed on day 10. (A) Autoradiograph of incorporated radioactivity into cellular proteins. Cells treated with each siRNA were labeled with $Na_2[^{35}S]O_4$ for 24 h and analyzed as described in Experimental procedures. Cellular proteins were separated by 2–15% gradient SDS–PAGE. The arrowhead indicates the signal that disappeared upon treatment with HSase. (B) Ratio of sulfate incorporation into HS, CS and N-glycans in cellular proteins. The amounts of incorporated sulfate into HS, CS and N-glycans were estimated on the basis of the radioactivity released after the treatment of cells or cellular proteins with HSase, CSase and PNGase F, respectively. The amount of total sulfate incorporation into proteins was determined by the precipitation of the proteins in the cell lysate with TCA. No siRNA, cells treated with no siRNA; control (100 nM), cells treated with 100 nM control siRNA; control (200 nM), cells treated with 200 nM control siRNA; PAPST1, cells treated with 100 nM *PAPST1* siRNA; PAPST2, cells treated with 100 nM *PAPST2* siRNA; PAPST1+PAPST2, cells treated with 100 nM *PAPST1* siRNA and 100 nM *PAPST2* siRNA.

On day 9 (i.e. 2 days after the third transfection), the cells were labeled with $Na_2[^{35}S]O_4$ for 24 h. Figure 5A shows the autoradiograph of the cellular proteins in the cell lysates.
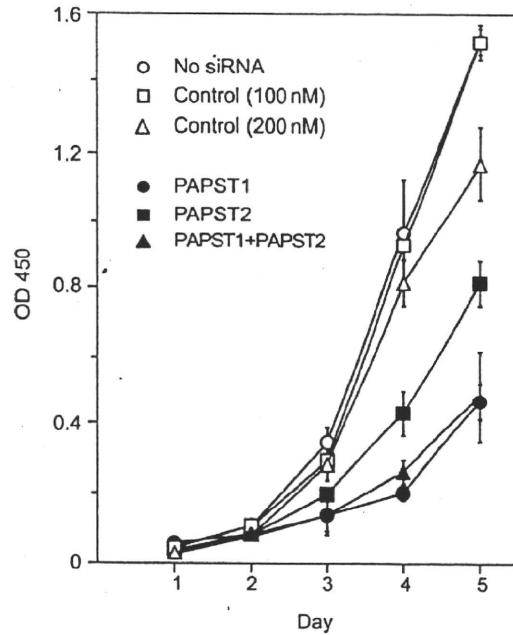
Fig. 6. Cellular proliferation of DLD-1 cells treated with siRNA. DLD-1 cells were transfected with each siRNA on days 1, 4 and 7 and seeded onto a 96-well plate on day 8. The number of cells was quantified once per day for 5 days using the WST-8 assay. No siRNA, cells treated with no siRNA; control (100 nM), cells treated with 100 nM control siRNA; control (200 nM), cells treated with 200 nM control siRNA; PAPST1, cells treated with 100 nM *PAPST1* siRNA; PAPST2, cells treated with 100 nM *PAPST2* siRNA; PAPST1+PAPST2, cells treated with 100 nM *PAPST1* siRNA and 100 nM *PAPST2* siRNA.

Treatment with either *PAPST1* or *PAPST2* siRNA reduced the density of HS (Figure 5A, arrowhead) and other signals. Figure 5B shows the sulfate incorporation into HS, CS, N-glycans and other glycans in the DLD-1 cells treated with each siRNA. The cells treated with *PAPST1* siRNA reduced the extent of sulfate incorporation into HS to one-third that of the cells treated with control siRNA. Treatment with *PAPST2* siRNA was less effective; the extent of sulfate incorporation into HS was half that of the cells treated with control siRNA. In the DLD-1 cells, treatment with *PAPST1* siRNA showed an effect on sulfation of HS, CS, and N-glycans, whereas treatment with *PAPST2* siRNA was mainly effective on HS (Figure 5B). These results indicate that gene expression of PAPS transporters regulates sulfation in this colorectal carcinoma cell line.

Gene silencing of PAPS transporters decreases cell growth in DLD-1 cells

Cellular proliferation of the siRNA-treated cells was further analyzed. On day 8 (i.e. 1 day after the third transfection), the siRNA-treated cells were seeded onto a 96-well plate and cell growth was measured once per day for 5 days using the WST-8 assay. Cells treated with either *PAPST1* or *PAPST2* siRNA showed significantly decreased cell growth relative to the cells treated with control siRNA (Figure 6). Similar to the result of sulfation, *PAPST1* siRNA was found to have a greater effect on cell growth than *PAPST2* siRNA in the DLD-1 cells.

The cell growth of double-knockdown cells was comparable to that of *PAPST1*-single knockdown cells. These results indicate that PAPS transporters play a role in the proliferation of colorectal carcinoma cells by controlling their sulfation status.
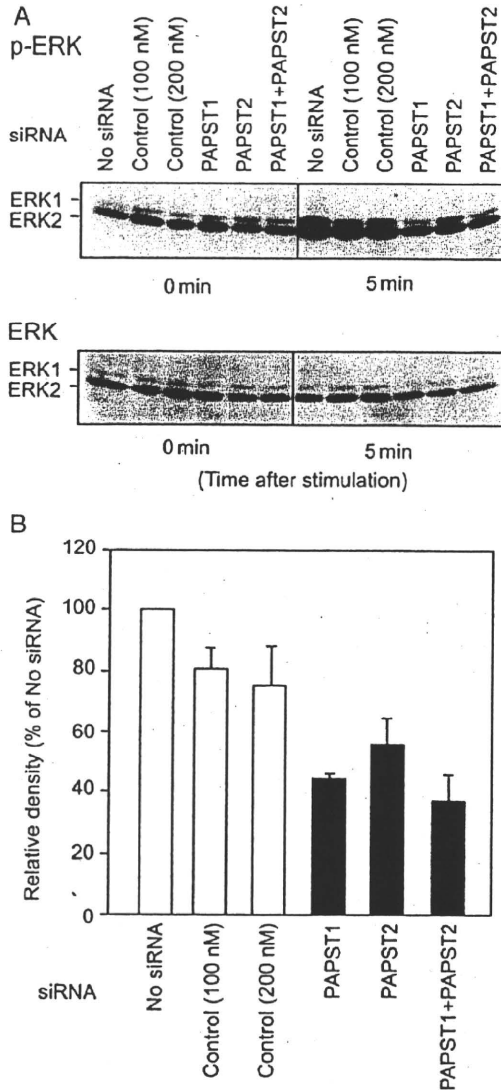

A
p-ERK

B

Fig. 7. FGF signaling of DLD-1 cells treated with siRNA. (**A**) Western blot analysis of ERK phosphorylation. DLD-1 cells were treated with each siRNA on days 1, 4 and 7 and stimulated with 10 ng/mL of FGF-2 on day 10. Cell lysates were prepared 0 and 5 min after stimulation and western blot analysis against ERK or phosphorylated ERK antibodies was performed. (**B**) Densitometric analysis of the western blot. Levels of phosphorylated ERK/ total ERK 5 min after stimulation were calculated using the NIH Image program and the value obtained from control cells is presented as 100%. Values shown are means (SDs) obtained from three independent experiments. No siRNA, cells treated with no siRNA; control (100 nM), cells treated with 100 nM control siRNA; control (200 nM), cells treated with 200 nM control siRNA; PAPST1, cells treated with 100 nM *PAPST1* siRNA; PAPST2, cells treated with 100 nM *PAPST2* siRNA; PAPST1+PAPST2, cells treated with 100 nM *PAPST1* siRNA and 100 nM *PAPST2* siRNA.

Gene silencing of PAPS transporters reduces HS-dependent growth factor signaling in DLD-1 cells

It is known that HS is involved in many growth-factor signaling pathways with interacting growth factors. FGF-2 is one of the HS-interacting growth factors and plays a role in regulating the proliferation of cells. Because the interaction between HS and FGF-2 requires the sulfation of HS (Rapraeger et al. 1991; Yayon et al. 1991), FGF-2 signaling was analyzed in the siRNA-treated DLD-1 cells. For this experiment, the DLD-1 cells treated with each siRNA were stimulated with 10 ng/mL FGF-2 on day 10 (i.e. 3 day after the third transfection), and the transduction of FGF signaling was assessed in terms of the phosphorylation of extracellular signal-regulated kinase (ERK). Western blots of phosphorylated ERK and total ERK in the siRNA-treated cells are shown in Figure 7A. In cells treated with either *PAPST1* or *PAPST2* siRNA, the ratio of phosphorylated ERK/total ERK was decreased relative to the cells treated with control siRNA (Figure 7B). The double-knockdown cells showed the lowest value for the ERK phosphorylation. The transduction of FGF signaling reflected the sulfation status of HS in the siRNA-treated DLD-1 cells. These results indicate that the expression of PAPS transporter genes affects HS-dependent growth factor signaling in colorectal carcinoma cells.

Discussion

The present study showed that the expression level of *PAPST1* is several times higher than that of *PAPST2* in colorectal carcinoma cell lines (Figure 1A). In colorectal carcinoma tissues, the difference in expression levels of two PAPS transporters was less prominent than the difference in the cell lines (Figure 1B). Immunohistochemical analyses revealed that PAPST1 protein is predominantly expressed in epithelial cells in both noncancerous and cancerous colorectal tissues (Figure 2E–I). The expression of PAPST1 was found to be remarkably increased in fibroblasts around invasive cancer cells (Figure 2I, asterisks) but did not change in epithelial carcinoma cells of cancerous colorectal tissues. In contrast, PAPST2 protein was strongly detected in epithelial cells in noncancerous colorectal tissues (Figure 2J), whereas the expression was faintly detectable in epithelial cells in cancerous colorectal tissues (Figure 2K). Therefore, the difference in the expression levels of PAPS transporters in colorectal carcinoma cell lines might be associated with decreased *PAPST2* expression in epithelial carcinoma cells.

Several studies have reported that the composition of sulfated glycoconjugates is altered in colorectal tissues during carcinogenesis. The sialyl 6-sulfo Le^x (Izawa et al. 2000) and 3′-sulfo-Le^a (Matsushita et al. 1995; Yamachika et al. 1997) epitopes are predominantly expressed in nonmalignant colorectal tissues, but are not detected in the malignant tissues. The impaired syntheses of sialyl 6-sulfo Le^x and disialyl Le^a upon malignant transformation are responsible for the accumulation of sialyl Le^x and sialyl Le^a in colon cancer cells (Izawa et al. 2000; Kannagi 2004; Miyazaki et al. 2004). Very recently, Yusa et al. (2010) reported that diminished transcription of sulfate transporter gene *DTDST* causes decreased expression of sialyl 6-sulfo Le^x and increased expression of sialyl Le^x in colon cancer cells. Sulfate transporters and PAPS synthases are

involved in PAPS synthesis, whereas PAPS transporters are required for sulfation reaction in the Golgi apparatus. The present study showed that the expression status of PAPS transporters is also a key factor in sulfation of cellular proteins in colon cancer cells. In addition, it has been shown that several sulfotransferases exhibit altered expression levels and activities in colorectal carcinomas (Vavasseur et al. 1994; Yang et al. 1994; Kuhns et al. 1995; Seko et al. 2002a, 2002b). Further identification of alterations of sulfated glycoconjugates and components involved in sulfation during malignancy will provide valuable insights into the role of sulfation in cancer.

Silencing of PAPS transporter genes influences sulfation of proteoglycans and proliferation of colorectal carcinoma cells. Dick et al. (2008) reported that the overexpression of PAPST1 enhances the sulfation of CS in the apical pathway of MDCK cells but does not affect HS sulfation. In contrast, the present work indicates that silencing of *PAPST1* gene expression in DLD-1 cells results in a decrease in both HS and CS sulfation (Figure 5). It is known that sulfotransferases for CS have higher K_m values for PAPS than the sulfotransferases for HS (Kolset et al. 2004). The results of the present study indicate that the sulfotransferases for HS are also susceptible to the levels of substrate in the Golgi apparatus in colorectal carcinoma cells.

Silencing of PAPS transporters reduces FGF-2 signaling in DLD-1 cells. It has been reported that both HS (Rapraeger et al. 1991; Yayon et al. 1991) and CS (Deepa et al. 2002) bind to FGF-2. Because the amount of cell surface HS was found to be more than three times greater than that of cell surface CS (Figure 3), HS is considered to contribute mainly to FGF-2 signaling in DLD-1 cells. Numerous studies have shown that cell surface HS plays a crucial role in normal growth and development. It is well known that HS is required for regulation of many growth factor-signaling pathways, such as FGF (Rapraeger et al. 1991; Yayon et al. 1991), wingless/Wnt (Reichsman et al. 1996), heparin-binding, epidermal growth factor-like growth factor (Aviezer and Yayon 1994), hepatocyte growth factor (Zioncheck et al. 1995) and vascular endothelial growth factor (Soker et al. 1994; Tessler et al. 1994). We previously demonstrated that PAPS transporters are essential for normal development in *Drosophila* (Kamiyama et al. 2003; Kamiyama and Nishihara 2004; Goda et al. 2006). Lüders et al. (2003) also demonstrated that the *Drosophila* ortholog of *PAPST1* is required for signaling of wingless and hedgehog. Therefore, alteration of HS sulfation may be a significant regulatory factor for cellular proliferation in colorectal carcinomas, although the significance of CS and other glycans should also be considered. Additionally, the strong expression of PAPST1 protein in fibroblasts in the vicinity of invasive cancer cells (Figure 2I, asterisks) suggests that PAPST1 has a role in the desmoplastic reaction during tumorigenesis to support cancer growth through modulation of HS-dependent signaling.

It has been reported that the expression of nucleotide sugar transporters is altered in the case of cancer or inflammation. In these studies, it was found that the expression level of a UDP-galactose transporter (SLC35A2) is increased in human colon carcinoma and is responsible for the synthesis of Thomsen–Friedenreich antigens and sialyl Le^a and sialyl Le^x

epitopes (Kumamoto et al. 2001). Expression of a GDP-fucose transporter (SLC35C1) is upregulated in hepatocellular carcinomas and plays a role in increased fucosylation (Moriwaki et al. 2007). In addition, the expression levels of transporters involved in sulfo sialyl Le^x glycan biosynthesis were coordinately upregulated by inflammation-related stimuli (Huopaniemi et al. 2004). Koike et al. (2004) reported that transcription of genes involved in the synthesis of the E-selectin ligands, namely fucosyltransferase VII, sialyltransferase ST3Gal-I and UDP-galactose transporter 1 (SLC35A2), is significantly induced in cancer cells under hypoxic culture conditions. Their study also showed that a hypoxia-inducible transcription factor induces transcription of these genes and leads to a significant increase in selectin-mediated cancer cell adhesion to endothelial cells (Koike et al. 2004). Furthermore, Yusa et al. (2010) suggested that the transcription of sulfate transporter *DTDST* is suppressed by epigenetic silencing via histone modification in colon cancer cells. It would be an interesting topic of research to elucidate how the expression of these transporter genes is transcriptionally regulated in cancer or inflammation.

Mutations in nucleotide sugar transporter genes responsible for several disorders have been recently identified (Lübke et al. 2001; Lühn et al. 2001; Martinez-Duncker et al. 2005; Hiraoka et al. 2007). With regard to the synthesis of GAGs, the mutation of a gene involved in the synthesis of CS, *SLC35D1*, was reported to be responsible for Schneckenbecken dysplasia, a severe skeletal dysplasia (Hiraoka et al. 2007). A missense mutation in the bovine *SLC35A3* gene, which encodes a UDP-*N*-acetylglucosamine transporter, causes complex vertebral malformation (Thomsen et al. 2006). To date, no disorders associated with PAPS transporter gene mutation have been reported. However, Clement et al. (2008) recently demonstrated that a zebrafish with a *PAPST1* mutation has cartilage defects that strongly resemble those seen in human patients with hereditary multiple exostoses. Additionally, analyses of *Drosophila* mutants demonstrated the significance of PAPS transporters in development (Kamiyama et al. 2003; Lüders et al. 2003; Goda et al. 2006). Our recent research has revealed that both PAPST1 and PAPST2 contribute to the maintenance and differentiation of mouse embryonic stem cells by regulating Wnt, bone morphogenetic protein and FGF signaling (Sasaki et al. 2009). The results of the present study provide additional information on the functions of PAPS transporters in cancer cells. In the future, approaches using transgenic or knockout mice would be helpful in elucidating the key roles of PAPS transporters.

Experimental procedures

Cell culture and tissue samples

Omega, DLD-1 and LS174T cell lines were cultured in Dulbecco's modified Eagle's medium (DMEM)/F12 (1:1) medium (Invitrogen Co., Carlsbad, CA), supplemented with 10% fetal bovine serum and 1× penicillin/streptomycin (Invitrogen).

The use of the clinical materials was approved by the ethical committee of the National Hospital Organization Osaka National Hospital, the Keio University Hospital, the

National Institute of Advanced Industrial Science and Technology, the Aichi Cancer Center Research Institute and Soka University. The formalin-fixed and paraffin-embedded colon cancer samples were obtained from the National Hospital Organization Osaka National Hospital and used for immunohistochemical analysis. The frozen rectal cancer samples were obtained from the Keio University Hospital and used for *in situ* hybridization. The frozen cancerous and non-cancerous colon tissues were obtained from the National Hospital Organization Osaka National Hospital and the Aichi Cancer Center Research Institute to use for quantitative PCR analysis.

Quantitative analysis of PAPST1 and PAPST2 transcripts

The quantities of *PAPST1* and *PAPST2* transcripts were determined using real-time PCR. Total RNA from human colorectal tissues was extracted using RNeasy Plus Mini (QIAGEN K.K., Tokyo, Japan) or the method of Chomczynski and Sacchi (1987). The features of each of the colorectal carcinoma samples were confirmed by histopathological examination (Table I). Total RNA from the cell lines was prepared using TRIzol reagent (Invitrogen). First-strand cDNA was synthesized with a Superscript II First Strand Synthesis kit (Invitrogen) with an oligo-dT primer. Real-time PCR was performed using qPCR Mastermix (QuickGoldStar; Eurogentec, Seraing, Belgium) and an ABI PRISM 7700 Sequence Detection System (Applied Biosystems, Foster, CA).

The PCR primer pair sequences and TaqMan probes used for each gene were same as those previously reported (Kamiyama et al. 2003, 2006). The relative amounts of *PAPST1* and *PAPST2* transcripts were normalized to the amount of glyceraldehyde 3-phosphate dehydrogenase (*GAPDH*) transcript present in the same cDNA.

In situ hybridization

A pBluescript SK(−) plasmid containing a 0.57 kb *PAPST1* sequence was linearized with *Not*I. A digoxigenin-labeled antisense riboprobe was synthesized with T7 RNA polymerase using Dig RNA Labeling Kits (Roche Applied Science, Indianapolis, IN). As a negative control, a sense riboprobe was synthesized with T3 RNA polymerase after linearization of the plasmid with *Xho*I.

Serial frozen sections prepared from rectal tissues in Tissue-Tech OCT compound (Sakura Finetechnical Co. Ltd., Tokyo, Japan) were thawed on slides and the OCT compound was removed. Sections were treated with 1 μg/mL of proteinase K at 37°C for 10 min and refixed in 4% paraformaldehyde at 4°C for 20 min. Sections were then pre-hybridized in hybridization buffer (5× SSC containing 50% deionized formamide, 10% dextran sulfate, 0.5% Tween 20, 5 mM dithiothreitol, 50 μg/mL of heparin and 50 μg/mL of yeast tRNA) and hybridized with a digoxigenin-labeled sense or antisense riboprobe in hybridization buffer at 58°C for 16 h. After hybridization, sections were sequentially washed with 5× SSC containing 50% formamide and 0.2% Tween-20 at 58°C for 30 min and three times with 2× SSC containing 50% formamide and 0.2% Tween-20 at 58°C for 30 min. The sections were then treated with 0.5% blocking buffer (Roche Applied Science) in TBST and reacted with alkaline phosphatase-

conjugated anti-digoxigenin antibody (Roche Applied Science). Endogenous phosphatases were inactivated with 2 mM levamisole in TBST and riboprobes were detected with 0.375 mg/mL of nitroblue tetrazolium, 0.175 mg/mL of 5-bromo-4-chloro-3-indolyl phosphate, 100 mM NaCl, 100 mM Tris–HCl, pH 9.5, 50 mM $MgCl_2$ and 0.1% Tween-20 for 2.5 h. The developed sections were washed three times with 10 mM Tris–HCl, pH 8.0, and 1 mM EDTA and were mounted with glycerol.

Immunohistochemical analysis

Rabbit polyclonal antibodies generated against mouse PAPST1, KAVPTEPPVQKV, and human PAPST2, CAKNPVRTYGYA, were purified by using each peptide and were then used to examine the immunohistochemical distribution of PAPS transporter proteins.

For immunostaining of formalin-fixed and paraffin-embedded tissue samples, 3 μm thick sections were serially cut and mounted on precoated slides. A Ventana system (Ventana XT system BenchMark; Ventana Medical Systems, Tucson, AZ) was used for immunohistochemical analysis. All procedures were performed automatically by the system according to the manufacturer's protocols. Briefly, the tissue sections were automatically treated with an antigen-retrieval solution (Ventana) and heated on a slide heater at 100°C for 30 min. Endogenous peroxidase activity was quenched by immersion in 3% hydrogen peroxide for 4 min. The sections were then incubated with anti-PAPST1 antibody (rabbit polyclonal, 1/500 dilution) for 30 min at 37°C. Detection was performed using the LSAB Ventana Iview DAB detection system according to the manufacturer's instructions. Sections were counterstained with hematoxylin.

For immunostaining of frozen tissue sections, the sections were fixed in cold acetone for 5 min and then rehydrated in phosphate-buffered saline (PBS). The sections were incubated with a blocking reagent (5% bovine serum albumin in PBS) at room temperature for 30 min and reacted with the anti-PAPST1 antibody (rabbit polyclonal, 1:500 dilution) or the anti-PAPST2 antibody (rabbit polyclonal, 1:100 dilution) at 4°C for 16 h. After washing with PBS, the sections were incubated with anti-rabbit immunoglobulin (IgG)-conjugated Alexa Fluor 488 at room temperature for 30 min. For counter staining, the sections were treated with phallotoxins conjugated Alexa Fluor 594 (Molecular Probes, Invitrogen, Eugene, OR) to stain the F-actin for 10 min and then incubated with Hoechst 33342 to stain the nucleus for 10 min. The sections were mounted in ProLong Gold Antifade reagent (Molecular Probes).

Verification of antibody specificity

The immunoreactivity of purified anti-PAPST1 antibody to human PAPST1 protein was confirmed by western blotting. The coding region of human PAPST1 was amplified by PCR using a forward primer 5′-GAATTCTGGACGCCAGATGG TGG-3′ and a reverse primer 5′-CTCGAGTCAAACCTT CTGCACAGGAG-3′. The PCR fragment was subcloned into the *Eco*RI and *Xho*I sites of the pCXN2-c-myc vector which contains an N-terminal-c-myc tag. HEK 293 cells were subcultured onto 6 cm dishes at a concentration of 1×10^6 cells/

243

dish and were transfected with 2 μg of plasmid using Lipofectamine 2000 reagent (Invitrogen). Three days after the transfection, cells were suspended in 120 μL of 10 mM triethanolamine containing 0.8 M Sorbitol and lysed with 60 μL of 3× SDS sample buffer (New England Biolabs Inc., Ipswich, MA) at 4°C for 16 h. The whole cell lysate (1 μg protein) was subjected to 10% SDS–polyacrylamide gel electrophoresis (PAGE), and proteins were transferred onto polyvinylidene difluoride membranes (Millipore). The membrane blot was blocked with 5% skimmed milk in PBS containing 0.1% Tween-20 (PBST, pH 7.4) and then was immunoreacted with the anti-PAPST1 antibody (1:5000 dilution in PBST) or an anti-c-myc monoclonal antibody (1:5000 dilution in PBST; Santa Cruz Biotechnology, Inc., Santa Cruz, CA). After washing with PBST, each blot was reacted with the corresponding secondary antibody conjugated with horseradish peroxidase in PBST. The blot was washed with PBST and developed with ECL Plus reagents (GE Healthcare Bioscience, Piscataway, NJ).

Metabolic labeling and determination of total sulfate incorporation into proteins

Twenty-four hours prior to analysis, cells were subcultured in a 24-well plate at a concentration of 1×10^5 cells/well in inorganic sulfate-free DMEM/F12 medium supplemented with 10% fetal bovine serum and 100 μCi/mL of carrier-free $Na_2[^{35}S]O_4$ (American Radiolabeled Chemicals Inc., St. Louis, MO). The cells were rinsed twice with PBS, suspended in 50 μL of lysis buffer (10 mM Tris–HCl, pH 7.4, 0.5% Nonidet P-40, 1 mM EDTA and 0.5 mM phenylmethylsulfonyl fluoride) and incubated on ice for 1 h. The solution was centrifuged at $18,500 \times g$ for 30 min, and the supernatant was used as the cell lysates. Twenty micrograms of the protein in each sample was precipitated with 10% TCA and washed with 5% TCA, followed by cold acetone. The precipitate was dried and dissolved in 50 μL of 0.5 N NaOH for scintillation counting.

Determination of sulfate incorporation into HS, CS and N-linked glycans

The $Na_2[^{35}S]O_4$-labeled cells were rinsed twice with PBS and cultured in normal medium for 2 h. Cells were rinsed with PBS and treated with 0.5 mL of DMEM/F12 medium containing 10 mU/mL of heparitinase (Seikagaku Kogyo, Tokyo, Japan) or 100 mU/mL of chondroitinase ABC (Seikagaku Kogyo) at 37°C for 2 h. The medium was saved and centrifuged at $18,500 \times g$ for 5 min, and the supernatant was used for scintillation counting. For each sample, the value was calculated as the difference between the radioactivity obtained from cells treated with the enzyme and the background radioactivity without the enzyme.

For quantification of sulfate incorporation into N-linked glycans, 20 μg of protein from the cell lysate was treated with PNGase F (New England BioLabs) at 37°C for 2 h. Proteins were precipitated with 20% TCA and washed with 5% TCA, followed by cold acetone. The precipitate was dried and dissolved in 50 μL of 0.5 N NaOH for scintillation counting. The value was calculated as the difference between the

radioactivity obtained from the cell lysate without the enzyme and the radioactivity from the cell lysate treated with the enzyme.

Treatment of DLD-1 cells with siRNA

Nineteen-base pair siRNAs with two bases of 3′ overhangs were designed using the siDirect program (http://genomics.jp/sidirect). The siRNA sequences used were as follows: for control siRNA, sense strand 5′-GUACCGCACGUCAUUCG UAUC-3′ and antisense strand 5′-UACGAAUGACGUGC GGUACGU-3′; for PAPST1 siRNA, sense strand 5′-GGU CAAGAGAGCAUAGGUAGG-3′ and antisense strand 5′-UA CCUAUGCUCUCUUGACCCC-3′; for PAPST2 siRNA, sense strand 5′-CCAGUUCGGACCUAUGGUUAU-3′ and antisense strand 5′-AACCAUAGGUCCGAACUGGAU-3′.

DLD-1 cells were subcultured onto 6 cm dishes at a concentration of 1×10^6 cells/dish 24 h prior to transfection. The cells were repeatedly transfected with 100 nM siRNA with Lipofectamine 2000 reagent three times on days 1, 4 and 7. On day 9, the cells were labeled with $Na_2[^{35}S]O_4$ for 24 h and analyzed as described in 'Metabolic labeling and determination of total sulfate incorporation into proteins'. RNA was extracted using TRIzol reagent (Invitrogen) on day 10.

Cell proliferation assay

Cell proliferation was assessed using an assay with a tetrazolium salt, 2-(2-methoxy-4-nitrophenyl)-3-(4-nitrophenyl)-5-(2,4-disulfophenyl)-2H tetrazolium monosodium salt (WST-8). In this experiment, cells were seeded onto a 96-well plate at a concentration of 2×10^3 cells/well in quadruplicate on day 8 and cultured in the normal medium. The number of cells was quantified once per day for 5 days using a Cell Counting Kit-8 (Dojindo Laboratories, Kumamoto, Japan). The absorbance at 450 nm was measured 2 h after the reaction using a microplate reader (Model 3550; Bio-Rad Labs, Hercules, CA). The obtained value was adjusted by subtracting the background value (obtained without the reagent).

Cell stimulation and western blot analysis

For activation of FGF signaling, cells were serum-starved for 16 h and treated with 10 ng/mL of FGF-2 (Upstate Biotechnology Inc., Lake Placid, NY) for 5 min. Cells were rinsed with ice-cold PBS and lysed in lysis buffer (50 mM Tris–HCl, pH 7.4; 150 mM NaCl, 1% Triton X-100, 1 mM Na_3VO_4, 10 mM NaF and protease inhibitors) and centrifuged at $18,500 \times g$ for 5 min. The supernatant was used for western blot analysis.

For western blot analysis, proteins in the cell lysate (5 μg) were separated with 10% SDS–PAGE and transferred onto polyvinylidene difluoride membranes (Millipore). The membrane blot was blocked with 1% bovine serum albumin in 20 mM Tris-buffered saline containing 0.1% Tween-20 (TBST, pH 7.4) for 2 h at room temperature and then immunoreacted with an antibody against ERK-1/2 (Cell Signaling Technology, Beverly, MA) or phosphorylated ERK-1/2 (Thr-202 and Thr-204; Cell Signaling Technology) in blocking buffer at 4°C overnight. After washing with TBST, each blot was reacted with its corresponding secondary antibody conjugated with

horseradish peroxidase in TBST at room temperature for 1 h. The blot was washed with TBST and developed with ECL Plus reagents (GE Healthcare Bioscience).

Funding

Acknowledgement

Conflict of interest statement

None declared.

Abbreviations

CS, chondroitin sulfate; DMEM, Dulbecco's modified Eagle's medium; ERK, extracellular signal-regulated kinase; FGF, fibroblast growth factor; GAG, glycosaminoglycan; GAPDH, glyceraldehyde 3-phosphate dehydrogenase; GDP, guanidine diphosphate; HS, heparan sulfate; IgG, immunoglobulin G; Le^a, galactose β 1-3[fucose α 1-4] N-acetylglucosamine; Le^x, galactose β 1-4[fucose α 1-3] N-acetylglucosamine; PAPS, 3'-phosphoadenosine 5'-phosphosulfate; PAGE, polyacrylamide gel electrophoresis; PBS, phosphate-buffered saline; PCR, polymerase chain reaction; PBST, PBS containing 0.1% Tween-20; PNGase, peptide:N-glycosidase; RNAi, RNA interference; siRNA, small interfering RNA; TBST, Tris-buffered saline containing 0.1% Tween-20; TCA, trichloroacetic acid; UDP, uridine diphosphate.

References

Aviezer D, Yayon A. 1994. Heparin-dependent binding and autophosphorylation of epidermal growth factor (EGF) receptor by heparin-binding EGF-like growth factor but not by EGF. *Proc Natl Acad Sci USA*. 91:12173–12177.

Chomczynski P, Sacchi N. 1987. Single-step method of RNA isolation by acid guanidinium thiocyanate–phenol–chloroform extraction. *Anal Biochem*. 162:156–159.

Clement A, Wiweger M, von der Hardt S, Rusch MA, Selleck SB, Chien CB, Roehl HH. 2008. Regulation of zebrafish skeletogenesis by ext2/dackel and papst1/pinscher. *PLoS Genet*. 4:e1000136.

Deepa SS, Umehara Y, Higashiyama S, Itoh N, Sugahara K. 2002. Specific molecular interactions of oversulfated chondroitin sulfate E with various heparin-binding growth factors. Implications as a physiological binding partner in the brain and other tissues. *J Biol Chem*. 277:43707–43716.

Dick G, Grødahl F, Prydz K. 2008. Overexpression of the 3'-phosphoadenosine 5'-phosphosulfate (PAPS) transporter 1 increases sulfation of chondroitin sulfate in the apical pathway of MDCK II cells. *Glycobiology*. 18:53–65.

Goda E, Kamiyama S, Uno T, Yoshida H, Ueyama M, Kinoshita-Toyoda A, Toyoda H, Ueda R, Nishihara S. 2006. Identification and characterization of a novel *Drosophila* 3'-phosphoadenosine 5'-phosphosulfate transporter. *J Biol Chem*. 281:28508–28517.

Hiraoka S, Furuichi T, Nishimura G, Shibata S, Yanagishita M, Rimoin DL, Superti-Furga A, Nikkels PG, Ogawa M, Katsuyama K, et al. 2007. Nucleotide-sugar transporter SLC35D1 is critical to chondroitin sulfate synthesis in cartilage and skeletal development in mouse and human. *Nat Med*. 13:1363–1367.

Huopaniemi L, Kolmer M, Niittymaki J, Pelto-Huikko M, Renkonen R. 2004. Inflammation-induced transcriptional regulation of Golgi transporters required for the synthesis of sulfo sLex glycan epitopes. *Glycobiology*. 14:1285–1294.

Irimura T, Wynn DM, Hager LG, Cleary KR, Ota DM. 1991. Human colonic sulfomucin identified by a specific monoclonal antibody. *Cancer Res*. 51:5728–5735.

Izawa M, Kumamoto K, Mitsuoka C, Kanamori C, Kanamori A, Ohmori K, Ishida H, Nakamura S, Kurata-Miura K, Sasaki K, et al. 2000. Expression of sialyl 6-sulfo Lewis X is inversely correlated with conventional sialyl Lewis X expression in human colorectal cancer. *Cancer Res*. 60:1410–1416.

Kamimura K, Fujise M, Villa F, Izumi S, Habuchi H, Kimata K, Nakato H. 2001. *Drosophila* heparan sulfate 6-*O*-sulfotransferase (*dHS6ST*) gene. Structure, expression, and function in the formation of the tracheal system. *J Biol Chem*. 276:17014–17021.

Kamimura K, Koyama T, Habuchi H, Ueda R, Masu M, Kimata K, Nakato H. 2006. Specific and flexible roles of heparan sulfate modifications in *Drosophila* FGF signaling. *J Cell Biol*. 174:773–778.

Kamiyama S, Nishihara S. 2004. The subcellular PAPS synthesis pathway responsible for the sulfation of proteoglycans: A comparison between humans and *Drosophila melanogaster*. *Trends Glycosci Glycotechnol*. 16:109–123.

Kamiyama S, Sasaki N, Goda E, Ui-Tei K, Saigo K, Narimatsu H, Jigami Y, Kannagi R, Irimura T, Nishihara S. 2006. Molecular cloning and characterization of a novel 3'-phosphoadenosine 5'-phosphosulfate transporter, PAPST2. *J Biol Chem*. 281:10945–10953.

Kamiyama S, Suda T, Ueda R, Suzuki M, Okubo R, Kikuchi N, Chiba Y, Goto S, Toyoda H, Saigo K, et al. 2003. Molecular cloning and identification of 3'-phosphoadenosine 5'-phosphosulfate transporter. *J Biol Chem*. 278:25958–25963.

Kannagi R. 2004. Molecular mechanism for cancer-associated induction of sialyl Lewis X and sialyl Lewis A expression—the Warburg effect revisited. *Glycoconj J*. 20:353–364.

Koike T, Kimura N, Miyazaki K, Yabuta T, Kumamoto K, Takenoshita S, Chen J, Kobayashi M, Hosokawa M, Taniguchi A, et al. 2004. Hypoxia induces adhesion molecules on cancer cells: A missing link between Warburg effect and induction of selectin-ligand carbohydrates. *Proc Natl Acad Sci USA*. 101:8132–8137.

Kolset SO, Prydz K, Pejler G. 2004. Intracellular proteoglycans. *Biochem J*. 379:217–227.

Kuhns W, Jain RK, Matta KL, Paulsen H, Baker MA, Geyer R, Brockhausen I. 1995. Characterization of a novel mucin sulphotransferase activity synthesizing sulphated *O*-glycan core 1,3-sulphate-Gal β 1-3GalNAc α-R. *Glycobiology*. 5:689–697.

Kumamoto K, Goto Y, Sekikawa K, Takenoshita S, Ishida N, Kawakita M, Kannagi R. 2001. Increased expression of UDP-galactose transporter messenger RNA in human colon cancer tissues and its implication in synthesis of Thomsen-Friedenreich antigen and sialyl Lewis A/X determinants. *Cancer Res*. 61:4620–4627.

Lin X, Buff EM, Perrimon N, Michelson AM. 1999. Heparan sulfate proteoglycans are essential for FGF receptor signaling during *Drosophila* embryonic development. *Development*. 126:3715–3723.

Lin X, Perrimon N. 1999. Dally cooperates with *Drosophila* Frizzled 2 to transduce Wingless signalling. *Nature*. 400:281–284.

Lübke T, Marquardt T, Etzioni A, Hartmann E, von Figura K, Köner C. 2001. Complementation cloning identifies CDG-IIc, a new type of congenital disorders of glycosylation, as a GDP-fucose transporter deficiency. *Nat Genet*. 28:73–76.

Lüders F, Segawa H, Stein D, Selva EM, Perrimon N, Turco SJ, Häcker U. 2003. *Slalom* encodes an adenosine 3'-phosphate 5'-phosphosulfate transporter essential for development in *Drosophila*. *EMBO J*. 22:3635–3644.

Lühn K, Wild MK, Eckhardt M, Gerardy-Schahn R, Vestweber D. 2001. The gene defective in leukocyte adhesion deficiency II encodes a putative GDP-fucose transporter. *Nat Genet*. 28:69–72.

Martinez-Duncker I, Dupre T, Piller V, Piller F, Candelier JJ, Trichet C, Tchernia G, Oriol R, Mollicone R. 2005. Genetic complementation reveals

245

a novel human congenital disorder of glycosylation of type II, due to inactivation of the Golgi CMP-sialic acid transporter. *Blood.* 105:2671–2676.

Matsushita Y, Yamamoto N, Shirahama H, Tanaka S, Yonezawa S, Yamori T, Irimura T, Sato E. 1995. Expression of sulfomucins in normal mucosae, colorectal adenocarcinomas, and metastases. *Jpn J Cancer Res.* 86:1060–1067.

Mitsuoka C, Sawada-Kasugai M, Ando-Furui K, Izawa M, Nakanishi H, Nakamura S, Ishida H, Kiso M, Kannagi R. 1998. Identification of a major carbohydrate capping group of the L-selectin ligand on high endothelial venules in human lymph nodes as 6-sulfo sialyl Lewis X. *J Biol Chem.* 273:11225–11233.

Miyazaki K, Ohmori K, Izawa M, Koike T, Kumamoto K, Furukawa K, Ando T, Kiso M, Yamaji T, Hashimoto Y, et al. 2004. Loss of disialyl Lewis(a), the ligand for lymphocyte inhibitory receptor sialic acid-binding immunoglobulin-like lectin-7 (Siglec-7) associated with increased sialyl Lewis(a) expression on human colon cancers. *Cancer Res.* 64:4498–4505.

Moriwaki K, Noda K, Nakagawa T, Asahi M, Yoshihara H, Taniguchi N, Hayashi N, Miyoshi E. 2007. A high expression of GDP-fucose transporter in hepatocellular carcinoma is a key factor for increases in fucosylation. *Glycobiology.* 17:1311–1320.

Nakamori S, Kameyama M, Imaoka S, Furukawa H, Ishikawa O, Sasaki Y, Kabuto T, Iwanaga T, Matsushita Y, Irimura T. 1993. Increased expression of sialyl Lewisx antigen correlates with poor survival in patients with colorectal carcinoma: Clinicopathological and immunohistochemical study. *Cancer Res.* 53:3632–3637.

Nakayama T, Watanabe M, Katsumata T, Teramoto T, Kitajima M. 1995. Expression of sialyl Lewis(a) as a new prognostic factor for patients with advanced colorectal carcinoma. *Cancer.* 75:2051–2056.

Rapraeger AC, Krufka A, Olwin BB. 1991. Requirement of heparan sulfate for bFGF-mediated fibroblast growth and myoblast differentiation. *Science.* 252:1705–1708.

Reichsman F, Smith L, Cumberledge S. 1996. Glycosaminoglycans can modulate extracellular localization of the wingless protein and promote signal transduction. *J Cell Biol.* 135:819–827.

Sasaki N, Hirano T, Ichimiya T, Wakao M, Hirano K, Kinoshita-Toyoda A, Toyoda H, Suda Y, Nishihara S. 2009. The 3′-phosphoadenosine 5′-phosphosulfate transporters, PAPST1 and 2, contribute to the maintenance and differentiation of mouse embryonic stem cells. *PLoS ONE.* 4: e8262.

Seko A, Nagata K, Yonezawa S, Yamashita K. 2002a. Ectopic expression of a GlcNAc 6-O-sulfotransferase, GlcNAc6ST-2, in colonic mucinous adenocarcinoma. *Glycobiology.* 12:379–388.

Seko A, Nagata K, Yonezawa S, Yamashita K. 2002b. Down-regulation of Gal 3-O-sulfotransferase-2 (Gal3ST-2) expression in human colonic nonmucinous adenocarcinoma. *Jpn J Cancer Res.* 93:507–515.

Soker S, Goldstaub D, Svahn CM, Vlodavsky I, Levi BZ, Neufeld G. 1994. Variations in the size and sulfation of heparin modulate the effect of heparin on the binding of VEGF165 to its receptors. *Biochem Biophys Res Commun.* 203:1339–1347.

Tessler S, Rockwell P, Hicklin D, Cohen T, Levi BZ, Witte L, Lemischka IR, Neufeld G. 1994. Heparin modulates the interaction of VEGF165 with soluble and cell associated flk-1 receptors. *J Biol Chem.* 269: 12456–12461.

Thomsen B, Horn P, Panitz F, Bendixen E, Petersen AH, Holm LE, Nielsen VH, Agerholm JS, Arnbjerg J, Bendixen C. 2006. A missense mutation in the bovine *SLC35A3* gene, encoding a UDP-*N*-acetylglucosamine transporter, causes complex vertebral malformation. *Genome Res.* 16:97–105.

Tsuiji H, Hayashi M, Wynn DM, Irimura T. 1998a. Expression of mucin-associated sulfo-Lea carbohydrate epitopes on human colon carcinoma cells. *Jpn J Cancer Res.* 89:1267–1275.

Tsuiji H, Hong JC, Kim YS, Ikehara Y, Narimatsu H, Irimura T. 1998b. Novel carbohydrate specificity of monoclonal antibody 91.9H prepared against human colonic sulfomucin: Recognition of sulfo-Lewis(a) structure. *Biochem Biophys Res Commun.* 253:374–381.

Vavasseur F, Dole K, Yang J, Matta KL, Myerscough N, Corfield A, Paraskeva C, Brockhausen I. 1994. O-glycan biosynthesis in human colorectal adenoma cells during progression to cancer. *Eur J Biochem.* 222:415–424.

Yamachika T, Nakanishi H, Inada K, Kitoh K, Kato T, Irimura T, Tatematsu M. 1997. Reciprocal control of colon-specific sulfomucin and sialosyl-Tn antigen expression in human colorectal neoplasia. *Virchows Arch.* 431:25–30.

Yamori T, Ota DM, Cleary KR, Hoff S, Hager LG, Irimura T. 1989. Monoclonal antibody against human colonic sulfomucin: Immunochemical detection of its binding sites in colonic mucosa, colorectal primary carcinoma, and metastases. *Cancer Res.* 49:887–894.

Yang JM, Byrd JC, Siddiki BB, Chung YS, Okuno M, Sowa M, Kim YS, Matta KL, Brockhausen I. 1994. Alterations of O-glycan biosynthesis in human colon cancer tissues. *Glycobiology.* 4:873–884.

Yayon A, Klagsbrun M, Esko JD, Leder P, Ornitz DM. 1991. Cell surface, heparin-like molecules are required for binding of basic fibroblast growth factor to its high affinity receptor. *Cell.* 64:841–848.

Yusa A, Miyazaki K, Kimura N, Izawa M, Kannagi R. 2010. Epigenetic silencing of the sulfate transporter gene *DTDST* induces sialyl Lewisx expression and accelerates proliferation of colon cancer cells. *Cancer Res.* 70:4064–4073.

Zioncheck TF, Richardson L, Liu J, Chang L, King KL, Bennett GL, Fugedi P, Chamow SM, Schwall RH, Stack RJ. 1995. Sulfated oligosaccharides promote hepatocyte growth factor association and govern its mitogenic activity. *J Biol Chem.* 270:16871–16878.

ORIGINAL ARTICLE

Predictive factors for the effectiveness of neoadjuvant chemotherapy and prognosis in triple-negative breast cancer patients

Hiroko Masuda · Norikazu Masuda · Yoshinori Kodama · Masami Ogawa ·
Michiko Karita · Jun Yamamura · Kazunori Tsukuda · Hiroyoshi Doihara ·
Shinichiro Miyoshi · Masayuki Mano · Shoji Nakamori · Toshimasa Tsujinaka

Abstract

Purpose Triple-negative breast cancers (TNBCs) do not derive benefit from molecular-targeted treatments such as endocrine therapy or anti-HER2 therapy because they lack those molecular targets. On the other hand, TNBCs have been shown to respond to neoadjuvant chemotherapy (NAC). In this study, we analyzed TNBC patients who were treated with NAC at Osaka National Hospital over a recent 5-year period to clarify the predictive factors for NAC and prognostic factors.

Patients and methods Thirty-three TNBC patients underwent sequential NAC with anthracycline (FEC100: 5FU 500 mg/m^2, epirubicin 100 mg/m^2, and cyclophosphamide 500 mg/m^2/q3w, 4 courses) and taxanes (paclitaxel 80 mg/m^2/qw, 12 courses or docetaxel 75 mg/m^2/q3w, 4 courses)

from May 2003 to July 2008. Pre-therapeutical and surgical specimens were studied for expressions of ER, PgR, HER-2, EGFR, cytokeratin 5/6, Ki-67, p53 and androgen receptor by immunohistochemistry (IHC). We analyzed clinicopathological factors and molecular markers in regard to the response to NAC and prognosis.

Results Pathological complete response (pCR) was achieved in 12 TNBC patients (36%). The pCR rate in the basal-like phenotype was significantly lower than in the non-basal-like phenotype (23 vs. 64%, respectively: $P = 0.02$). High pre-operative expressions of Ki-67 ($\geq$50%) and HER-2 (2+) were considered as predictive factors for a better response from NAC. Pre-operative Ki-67 expression showed a significant correlation with disease-free survival (DFS) and a lower expression of Ki-67 (<50%) after NAC was favorable for DFS among non-pCR patients.

Conclusions A non-basal-like phenotype and higher expressions of Ki-67 and HER-2 (2+) were favorable factors for NAC. However, a higher expression of Ki-67 on the surgical specimen after NAC was also a poor prognostic factor.

H. Masuda · N. Masuda · M. Ogawa · M. Karita · J. Yamamura ·
S. Nakamori · T. Tsujinaka
Department of Surgery,
National Hospital Organization Osaka National Hospital,
Osaka, Japan

Y. Kodama · M. Mano
Department of Pathology,
National Hospital Organization Osaka National Hospital,
Osaka, Japan

H. Masuda (✉) · K. Tsukuda · H. Doihara · S. Miyoshi
Department of Cancer and Thoracic Surgery,
Okayama University Graduate School of Medicine,
Dentistry and Pharmaceutical Sciences,
2-5-1 Shikatacho Kitaku,
Okayama 700-8558, Japan
e-mail: masuhiro123@hotmail.com

Abbreviations

TNBC	Triple negative breast cancer
NAC	Neoadjuvant chemotherapy
pCR	Pathological complete response
ER	Estrogen receptor
PgR	Progesterone receptor
AR	Androgen receptor
EGFR	Epidermal growth factor receptor
CK	Cytokeratin

Introduction

Triple-negative breast cancers (TNBCs) are characterized by the lack of expression of estrogen receptor (ER), progesterone receptor (PR), and human epidermal growth factor receptor 2 (HER-2). These cancers occur in ~20–25% of all breast cancers and are associated with an unfavorable prognosis. They derive no benefit from molecularly targeted treatments such as endocrine therapy or trastuzumab [1]. Therefore, identifying appropriate treatments for TNBC is an important issue.

Recent precise gene expression analysis revealed that TNBC is a heterogeneous group of tumors. One of the subgroups is a basal-like subtype, which is characterized by similar gene expression as the basal/myoepithelial cells of the normal breast [1–5]. Basal-like breast cancer has also been identified with immunohistochemical (IHC) staining of basal markers, such as cytokeratins (CKs) and epithelial growth factor receptor (EGFR). TNBCs without these basal markers are classified as non-basal-like subtypes, which are rare breast cancers, and classifications based on gene expression have not been clarified yet. Non-basal-like tumors are also reported to have a better prognosis than basal-like phenotypes [6, 7]. Because of the lack of targeted therapies and their aggressive clinical behaviors, TNBCs are relevant groups to be investigated for their characteristics. Though TNBCs are considered to have poor prognosis generally, TNBCs have been shown to be chemosensitive.

Neoadjuvant chemotherapy (NAC) in primary breast cancers has been shown to produce an outcome equivalent to that of adjuvant chemotherapy [8, 9]. Patients who show a pathological complete response (pCR) in the primary tumors after NAC have a better prognosis [10]. The pathological responses are important prognostic parameters and can be used as surrogate parameters for clinical outcome, so we analyzed the effects of clinicopathological factors as well as immunohistochemical factors on pathological responses after NAC. However, the paradox that TNBC and HER-2 positive subtypes showed higher chemosensitivity but worse survival due to higher relapse after chemotherapy is also known well [10, 11].

Several biological markers have been proposed as prognostic characteristics in breast cancers. ER, PR and HER-2 are such biological markers as well as being therapeutic markers and Ki-67, p53 and androgen receptor (AR) are shown to be associated with prognosis [12–16]. AR is known to be present in the majority of primary and metastatic invasive breast tumors and is often co-expressed with ER and PR in these tumors. Though little is known about the role of AR in hormonal response, AR expression has been shown to be associated with a better outcome for untreated breast cancer patients [14]. Ki-67 is a nuclear antigen expressed in the G1, S, and G2 phases but not in the

G0 or resting phase of the cell cycle. Ki-67 has been established as a proliferation marker in breast cancers and high proliferation activity has been found to have predictive value for the response to NAC [17]. Also p53 expression status has been used as a predictive factor for response to systemic therapy, because tumor cells with non-functional p53 do not respond to systemic therapy due to a failure in apoptosis [13, 15].

Because chemotherapy is the only treatment other than surgery for TNBC, the definition of clinical markers in regard to chemotherapeutic response and prognosis is very important. However, there are still few studies focusing on TNBC. In this study, we analyzed clinicopathological factors, phenotypes, and molecular markers of TNBC in regard to the response to NAC and prognosis.

Patients and methods

Patients and neoadjuvant chemotherapy

One hundred and 63 breast cancer patients underwent NAC with a sequential regimen containing anthracycline (FEC100: 5FU 500 mg/m^2, epirubicin 100 mg/m^2, cyclophosphamide 500 mg/m^2/q3w, 4 courses) and taxanes (paclitaxel 80 mg/m^2/qw, 12 courses or docetaxel 75 mg/m^2/q3w, 4 courses) at Osaka National Hospital (Osaka, Japan) from May 2003 to July 2008. The criteria for entry were invasive breast cancer patients from 20 to 70 years old with any T and N0-2 disease, who were diagnosed histologically, were absent from distant metastasis and with normal organ functions. Thirty-three patients (20%) among 163 breast cancer patients were identified as TNBCs. The clinical evaluation of the response to NAC was determined by clinical findings, CT and MRI examinations according to RECIST. All patients were included in clinical trials approved by an institutional review board and asked for written informed consent.

Immunohistochemistry

Pre-therapeutical specimens were obtained by the 14G-needle biopsy in all cases and pathological examinations using standard hematoxylin and eosin staining were carried out. Immunohistochemical evaluation for ER, PgR, HER-2, EGFR, CK5/6, Ki-67, p53 and AR in tissue sections were detected using antibodies (ER:Cat.No. 760-2596I, PgR: 760-2816, HER-2:760-2901, EGFR:790-2988, CK5/6:960-4253, Ki-67:760-2910, p53:760-2912, Ventana Japan, Yokohama, Japan, AR:M3562, Dako Japan, Tokyo, Japan). Visualization of the bound antibodies was performed using a DAKO EnvisionTM + System (Dako Japan Inc., Tokyo, Japan) according to the manufacturer's instructions. Positive

cell rates (%) of ER and PgR were determined as a ratio of positive cells to total cancer cells and a value of 10% or higher were rated as positive [18, 19]. HER-2 expression was defined as (0) to (3+) based on positive cell rates and the intensity of IHC staining. Tumors showing weak over-expression (2+) of HER-2 were also tested by the fluorescence in situ hybridization (FISH) method to clarify the gene amplification of the HER-2 gene. The HER-2 gene is visualized as green fluorescent grains and a control of centromere 17 is visualized as orange fluorescent grains (Path Vysion, Abbott, IL, USA). Thus, HER-2 positives were either strong positives (3+) from IHC or positive for gene amplification from FISH analysis.

TNBCs are negative for ER, PgR and HER-2 as described earlier. Among TNBCs with 1–9% of ER and/or PgR expression were defined as hormone receptor (HR) weak and analyzed separately. TNBCs with HER-2 (2+) and that were FISH negative were also analyzed separately.

Proliferative activity was determined by IHC for the Ki-67 antibody. Ki-67 values were expressed as the percentage of positive cell counts among at least 100 tumor cells in each case. Patients with positive staining of Ki-67 at 50% or more were defined as high Ki-67 patients. AR and p53 were defined as positive if tumor cells showed positive staining regardless of rate. Basal-like subtype was defined as CK5/6 positive and/or EGFR positive in 5% or more cells.

Surgical treatment

All patients underwent surgical treatment after NAC. Breast conservative therapy or a mastectomy with or without axillary dissection was performed according to the decision of the surgeons' conference. Surgical specimens were histologically analyzed again, and the pathological response for NAC was evaluated. When no residual invasive tumor cells were found, tumors were identified as pathological complete response (pCR). Surgical specimens from non-pCR patients were analyzed for expressions of Ki-67, p53 and AR as described earlier.

Statistics

A univariate analysis of the pCR rate was carried out by the χ^2 test, and a multivariate analysis was done by multiple logistic regression analysis. The patients' survival was calculated from the first date of treatment until the date of death or the end of follow-up. A univariate analysis of disease-free survival (DFS) was done using the Kaplan–Meier method with a log-rank test, and a multivariate disease survival analysis was carried out under the Cox proportional hazards model. All data were analyzed with JMP for Windows (SAS Institute, Tokyo, Japan).

Results

Relationship between pCR and clinicopathological factors

Thirty-three patients were identified as TNBCs, and the patients' data are shown in Table 1. The age of the patients ranged from 30 to 68 years old (median 50.0) and 21 patients had clinically positive nodes. Clinical response after NAC was rated as clinical complete response for 14 patients (42%), a clinical partial response for 14 patients (42%), a clinical stable disease for 3 patients (9%), and as a clinical progress disease for 2 patients (6%). Also pCR was achieved in only 12 patients (36%).

The correlations between clinicopathological factors such as tumor size, lymph nodal metastasis, age, histological grade, and pCR rate were analyzed (Table 2). However,

Table 1 Patients' characteristics

Variables	No (%)
Total	33
Age: years-old	30–68 (50 ± 11.1)
Histology	
Papillo-tubular	4 (12)
Solid tubular	14 (42)
Schirrous	11 (33)
Special type	4 (13)
T	
1	1 (3)
2	24 (72)
3	6 (18)
4	2 (6)
N	
0	12 (36)
1	17 (52)
2	4 (12)
Histological grade	
1	1 (3)
2	4 (12)
3	27 (81)
Unknown	1 (3)
HER-2	
0	18 (55)
1+	11 (33)
2+	4 (12)
HR (hormone receptor)	
Negative	26 (79)
Weak	7 (21)

T and N were defined by the criteria of UICC-breast

HR weak is a tumor with low levels of ER and/or PgR determined by IHC (1–9% weakly positive cells)

Table 2 pCR ratio based on clinicopathologic and immunohisto-chemistrical factors

Variables	Number (%)	pCR (%)	P volume	Odd
Age (years old)				
<50	18 (55)	6 (33)	0.69	
50≤	15 (45)	6 (40)		
Size (cm)				
<5	25 (76)	11 (44)	0.09	5.5
5≤	8 (24)	1 (13)		
N				
Positive	21 (64)	8 (38)	0.78	
Negative	12 (36)	4 (33)		
Histological grade				
1–2	5 (15)	3 (60)	0.26	
3	27 (84)	9 (33)		
HR				
Negative	26 (79)	10 (38)	0.95	
Weak	7 (21)	2 (28)		
HER-2				
0, 1+	29 (88)	9 (31)	0.08	6.67
2+	4 (12)	3 (75)		
p53				
Positive	21 (64)	8 (38)	0.78	
Negative	12 (36)	4 (33)		
Ki-67				
50≤ (high)	20 (61)	10 (50)	*0.04	5.5
<50 (low)	13 (39)	2 (15)		
AR				
Positive	6 (18)	3 (50)	0.45	
Negative	27 (82)	9 (33)		
Basal-like[#]				
Positive	22 (67)	5 (23)	*0.02	5.9
Negative	11 (33)	7 (64)		
CK5/6				
Positive	14 (42)	2 (14)	*0.02	
Negative	19 (58)	10 (53)		
EGFR				
Positive	18 (55)	4 (22)	0.06	
Negative	15 (45)	8 (53)		

* Statistically significant

[#] Basal-like subtype is defined as CK5/4 positive and/or EGFR positive. Thus, CK5/6 was not used for multivariate analysis

these clinicopathological factors did not show any correlation with the pCR rate.

Relationship between pCR, and molecular markers

Next, the correlation between molecular markers and the pCR rate was also analyzed. HER-2 (2+) tended to show a higher pCR rate than HER-2 negative (0 or 1+; 75 and 31%, respectively). In this study, basal markers of CK5/6 and EGFR were evaluated with 22 of 33 patients (67%) diagnosed with basal-like phenotype, and eleven patients (33%) diagnosed with the non-basal-like phenotype. The pCR rate for the basal-like phenotype was significantly lower than in the non-basal-like phenotype (23 and 64%, respectively: $P = 0.02$; Table 2). Ki-67 was also considered as a predictive factor for NAC response, because the pCR rate reaches 50% among high Ki-67 (≥50%) patients, while it was 15% in low Ki-67 patients ($P = 0.04$). The expressions of HR, p53 and AR were not correlated with pCR in this study. Multivariate analysis showed that only high Ki-67 was a significant factor for the prediction of pCR (Table 3). The classification of basal-like or non-basal-like phenotypes was negative for multivariate analysis, probably because high Ki-67 and non-basal-like were strongly correlated with each other; high Ki-67 accounted for 33% in the basal-like and 75% in the non-basal-like phenotype.

Relationship between pCR and disease-free survival

All patients underwent surgical resection after NAC and non-pCR patients were histologically evaluated. The average observation period after surgery was 2 years and eight patients (24%) showed distant metastasis during the observation period. Seven out of 8 patients had been defined as non-pCR and only one patient obtained pCR after NAC. Non-pCR patients showed a worse DFS compared with pCR patients, but it was not statistically significant (Fig. 1a). Basal-like phenotype and other clinicopathological factors such as age, tumor size and lymph nodal involvement failed to show a correlation with DFS (Table 4). Ki-67 before NAC showed a significant correlation with DFS and high Ki-67 patients showed a poor prognosis (Fig. 1b).

Disease-free survival among non-pCR patients

Among non-pCR patients, only 7 patients (29%) showed a recurrence. We analyzed clinicopathological and IHC factors for better prognosis among non-pCR patients. The immunohistological changes of tumors after NAC were

Table 3 Multivariate analysis of pCR and immunopathological factors

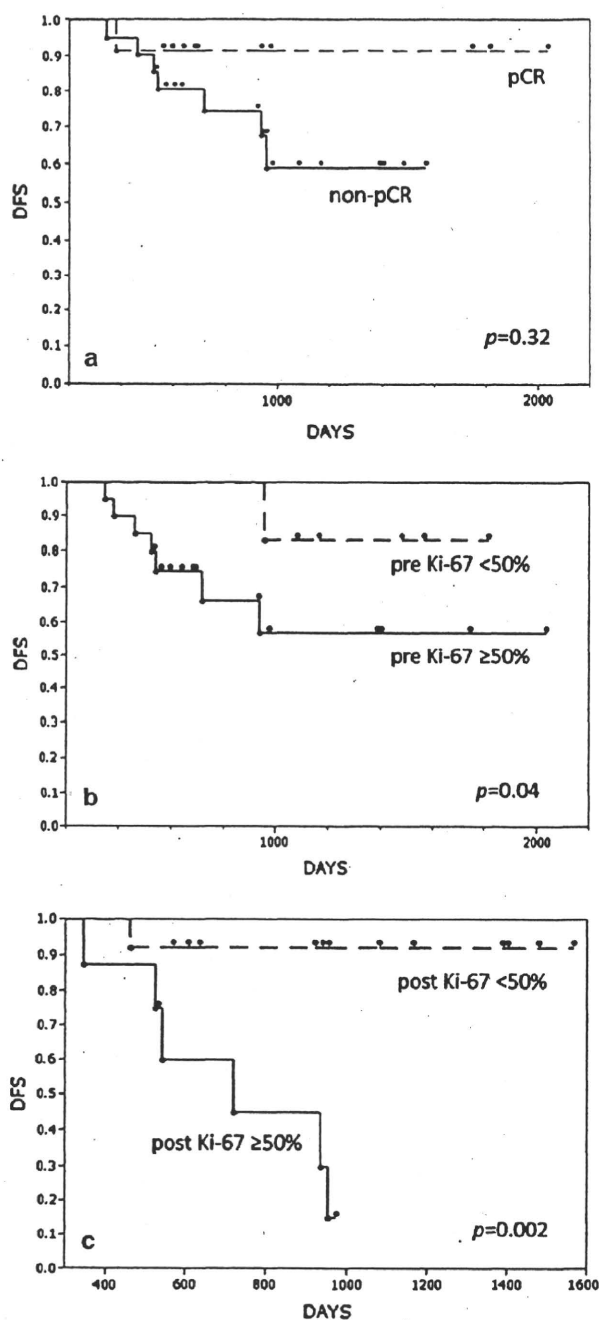| Variables	Odds	P value
Non-basal-like	3.9	0.13
HER2 (2+)	10.2	0.12
High Ki-67	8.4	0.03*

* Statistically significant

Fig. 1 Disease-free survival (DFS). **a** DFS of pCR and non-pCR patients after NAC. Non-pCR patients showed worse disease-free survival compared with pCR patients, but it was not statistically significant ($P = 0.32$). **b** DFS based on Ki-67 expression of pre-chemotherapy. High Ki-67 ($\geq 50\%$) patients showed significantly worse disease-free survival than low Ki-67 ($<50\%$) patients ($P = 0.04$). **c** DFS based on Ki-67 expression of post-NAC among non-pCR patients. Non-pCR patients who had high Ki-67 expression after NAC showed a poor prognosis ($P = 0.002$)

evaluated. Among non-pCR patients, 10 patients showed high Ki-67 before chemotherapy and 7 patients still showed high Ki-67 after NAC (Table 5). Among these patients, 6

Table 4 Multivariate analysis of disease-free survival and patients' characteristics

Variables	Hazard ratio	P value
≥ 50 years-old	0.39	0.2
≥ 5 cm	2.2	0.3
N positive	4.2	0.11
HR positive	3.2	0.1
HER-2 (2+)	3.2	0.56
Non-basal	1.4	0.6
High Ki-67	5.95	0.04*
p53 positive	0.48	0.3
AR positive	0.000	0.054
Non-pCR	3.7	0.16
High Ki-67 post-NAC[#]	13.2	0.0029*

[#] Data among non-pCR patients

* Statistically significant

Table 5 The correlation between Ki-67 expression, pCR and the change of Ki-67 expression among non-pCR patients

TNBC ($n = 33$)	Non-pCR		pCR
	Post-NAC Ki-67		
	High	Low	
Pre-NAC Ki-67			
High	7	3	10
Low	1	10	2

showed a recurrence and Ki-67 values after NAC were significantly correlated with DFS (Fig. 1c). The expressions of p53 and AR after NAC were not correlated with DFS (data not shown).

Discussion

TNBC is defined by the lack of ER, PgR and HER-2 expression. Because targeted therapies are not useful, chemotherapy is the only systemic treatment option for TNBC [1–5]. Thus, a comprehensive examination of the clinical phenotypes of TNBCs which respond to chemotherapy is important. TNBCs are a heterogeneous group and generally divided into two subtypes; basal-like phenotype and non-basal-like phenotype [6]. The basal-like phenotype is characterized as having a high expression of keratins, laminin, and EGFR.

Many data indicated that the pCR rate is higher in TNBC compared with other phenotypes [10]. A pathological evaluation after NAC is very important because pCR after NAC indicates better survival [8, 9]. Our data showed the pCR rate in TNBCs was 36%, which is consistent with previous

reports which stated 22–45% [10, 20]. This study hypothesized that non-basal-like phenotype, HER-2 (2+), and high Ki-67 could be predictive factors for pCR achievement, but multivariate analysis revealed that only Ki-67 was a significant factor for the prediction of pCR. This is probably because the non-basal-like phenotype showed a significantly higher Ki-67 expression compared with the basal-like phenotype. This study is consistent with previous studies which showed that Ki-67 indicates proliferation and high level of proliferation activity are associated with chemosensitivity [14]. Additionally, there are many reports that showed that the basal-like phenotype has a positive correlation with pCR [20]. Rouzier et al. reported that basal-like subtypes were more sensitive to NAC than luminal and normal-like cancers, but normal-like subtypes classified based on gene expression profiles are quite different from non-basal-like phenotypes based on IHC, because normal-like subtypes involved 60% of ER positive samples. Because classification based on gene expression is difficult for clinical use, our data based on IHC classification are quite useful. There are some reports that non-basal-like tumors showed better prognosis than basal-like phenotypes [6, 7]. Though the pCR rate was significantly higher in non-basal-like tumors, there was no difference in DFS between the two groups in this study.

Our study failed to show the significant benefit of pCR on DFS. That is probably because of the small number of the patients included or the short duration after surgical treatment in this study. Most cases which showed a recurrence in such a short period were non-pCR patients, and the only recurrent case in the pCR group was a patient with an intraductal residual after NAC and who showed brain metastasis within a year. In this study, Ki-67 was the only significant factor which was proved to affect DFS. Pre-NAC high Ki-67 was a poor prognostic factor in spite of the positive correlation with pCR. The post-NAC status of Ki-67 was also correlated with recurrence. High Ki-67 expression post-NAC showed a very poor prognosis and low Ki-67 post-NAC showed better survival even in the non-pCR group. The contradiction of high Ki-67 tumors, which showed a high chemosensitivity and high pCR rate but poor prognosis, may indicate the diversity of these tumors. As shown in Table 4, most high Ki-67 patients who could not achieve pCR kept a high expression of Ki-67 after NAC. Tumors which maintained high Ki-67 expression may indicate that the cellular activity is not suppressed by NAC. All of these facts showed that high Ki-67 tumors should be divided into two groups: tumors which show a high sensitivity to current chemo-drugs and a good prognosis and the tumors which continue to have high cellular activity after NAC and show a poor prognosis. Further study is needed to find other treatments for the latter.

Though many reports defined 20–30% of Ki-67 labeling index as a threshold [21], 50% was used for categorization in this study because most TNBCs are positive for Ki-67 and a 50% threshold at 50% was shown to be useful to predict both chemosensitivity and prognosis in TNBC patients.

The prognosis of HER-2 positive breast cancer has been proved by the usage of trastuzumab. The criteria of HER-2 positive are defined as a strong positive IHC or gene amplification in FISH [22]. HER-2 (2+) breast cancers without gene amplification are generally included in TNBC but HER-2 (2+) breast cancers showed higher chemosensitivity in this study and HER-2 (3+) breast cancers have been reported to be chemosensitive. The criteria of HER-2 positivity might be a moot point if TNBCs with HER-2 (2+) show a different cancer biology from TNBCs with negative HER-2.

Less than 10% of hormone receptor positivity had been considered as uncertain endocrine responsiveness or potential resistance [18, 19]. Though tumors with less than 10% hormone receptor positivity were included in TNBCs, we classified those with 0% staining both ER and PgR as HR negative and those with 1–9% as HR weak in this study. But the expressions of HR were not correlated with pCR. Moreover, tumors with any ER positive staining of at least 1% are recommended to be treated with endocrine therapy in latest reports [21, 23]. The categories of highly endocrine responsive and incompletely endocrine responsive are not relevant to the decision for endocrine therapy, but those categories are still important for the decision of chemotherapy.

In this study, we found that the pCR rate for the non-basal-like phenotype was significantly higher than that in the basal-like phenotype, though that difference was negative for multivariate analysis. This is because the positivity of Ki-67 was higher in the non-basal-like phenotype tumors. These data based on classification by IHC are very interesting and informative in a clinical setting because there are some discrepancy between criteria by gene expression profiling and those by IHC. Some previous papers were confused about classification by gene expression and by IHC. Non-basal-like subtype is a term correlated with IHC classification and difficult to adapt to criteria of gene expression. There are few reports focused on the non-basal-like phenotype. Our data may insinuate that non-basal-like subtypes are well adaptive to current chemotherapy and basal-like subtypes need another therapeutic agent. Because our data was based on a small number of patients, further examinations based on IHC classification are needed.

Our study indicated that TNBCs which were found to be non-pCR with high Ki-67 expression after NAC had a poor prognosis. How to treat these TNBCs will be a most important subject for future study. Only chemotherapy is a

proven treatment for TNBCs, but chemotherapy based on anthracyclins and taxanes has not been shown to be enough. There are several studies which showed the efficacy of new chemotherapeutic agents such as carboplatin, bavasituzumab and poly (ADP-ribose) polymerase-1 (PARP-1) inhibitor in TNBCs [24–26]. Studies of NAC with these agents are expected to improve the treatment of TNBCs.

References

1. Dawson SJ, Provenzano E, Caldas C (2009) Triple negative breast cancers: clinical and prognostic implications. Eur J Cancer 45(Suppl 1):27–40
2. Rakha EA, El-Sayed ME, Green AR et al (2007) Prognostic markers in triple-negative breast cancer. Cancer 109:25–32
3. Kreike B, van Kouwenhove M, Horlings H et al (2007) Gene expression profiling and histopathological characterization of triple-negative/basal-like breast carcinomas. Breast Cancer Res 9:R65
4. Kuroda N, Ohara M, Inoue K et al (2009) The majority of triple-negative breast cancer may correspond to basal-like carcinoma, but triple-negative breast cancer is not identical to basal-like carcinoma. Med Mol Morphol 42:128–131
5. Pintens S, Neven P, Drijkoningen M et al (2009) Triple negative breast cancer: a study from the point of view of basal CK5/6 and HER-1. J Clin Pathol 62:624–628
6. Rakha EA, Elsheikh SE, Aleskandarany MA et al (2009) Triple negative Breast cancer: distinguishing between basal and nonbasal subtypes. Clin Cancer Res 15:2301–2310
7. Gluz O, Liedtke C, Gottschalk N et al (2009) Triple-negative breast cancer-current status and future directions. Ann Oncol 20:1913–1927
8. Fisher B, Bryant J, Wolmark N et al (1998) Effect of preoperative chemotherapy on the outcome of women with operable breast cancer. J Clin Oncol 16:2672–2685
9. Scholl SM, Fourquet A, Asselain B et al (1994) Neoadjuvant versus adjuvant chemotherapy in premenopausal patients with tumors considered too large for breast conserving surgery: preliminary results of a randomized trial:S6. Eur J Cancer 30A:645–652
10. Liedtke C, Mazouni C, Hess KR et al (2008) Response to neoadjuvant therapy and long-term survival in patients with triple-negative breast cancer. J Clin Oncol 26:1275–1281
11. Carey LA, Dees EC, Sawyer L et al (2007) The triple negative paradox: Primary tumor chemosensitivity of breast cancer subtypes. Clin Cancer Res 13:2329–2334
12. Abrial SC, Penault-Llorca F, Delva R et al (2005) High prognostic significance of residual disease after neoadjuvant chemotherapy: a retrospective study in 710 patients with operable breast cancer. Breast Cancer Res Treat 94:255–263
13. von Minckwitz G, Sinn HP, Raab G et al (2008) Clinical response after two cycles compared to HER2, Ki-67, p53, and bcl-2 in independently predicting a pathological complete response after preoperative chemotherapy in patients with operable carcinoma of the breast. Breast Cancer Res 10:R30
14. OgawaY Hai E, Matsumoto K et al (2008) Androgen receptor expression in breast cancer: relationship with clinicopathological factors and biomarkers. Int J Clin Oncol 13:431–435
15. Berns EM, Foekens JA, Vossen R et al (2000) Complete sequencing of TP53 predicts poor response to systemic therapy of advanced breast cancer. Cancer Res 60:2155–2162
16. Assersohn L, Salter J, Powles TJ et al (2003) Studies of the potential utility of Ki67 as a predictive molecular marker of clinical response in primary breast cancer. Breast Cancer Res Treat 82:113–123
17. Burcombe RJ, Makris A, Richman PI et al (2005) Evaluation of ER, PgR, HER2 and Ki-67 as predictors of response to neoadjuvant anthracycline chemotherapy for operable breast cancer. Br J Cancer 92:147–155
18. Harvey JM, Clark GM, Osborne K et al (1999) Estrogen receptor status by immunohistochemistry is superior to the ligand-binding assay for predicting response to adjuvant endocrine therapy in breast cancer. J Clin Oncol 17:1474–1481
19. Goldhirsh A, Glick JH, Gelber RD et al (2005) Meeting highlights: international expert consensus on the primary therapy of early breast cancer 2005. Ann Oncol 16:1569–1583
20. Rouzier R, Perou CM, Symmans WF et al (2005) Breast cancer molecular subtypes respond differently to preoperative chemotherapy. Clin Cancer Res 11:5678–5685
21. Goldhirsch A, Ingle JN, Gelber RD et al (2009) Thresholds for therapies: highlights of the St Gallen International expert consensus on the primary therapy of early breast cancer. Ann Oncol 20:1319–1329
22. Wolff AC, Hammond MEH, Schwartz JN et al (2007) American society of clinical oncology/College of American pathologists guideline recommendations of human epidermal growth factor receptors 2 testing in breast cancer. J Clin Oncol 25:118–145
23. Hammond ME, Hayes DF, Dowsett M et al (2010) American society of clinical oncology/College of American pathologists guideline recommendations for immunohistochemical testing and estrogen and progesterone receptors in breast cancer. J Clin Oncol 2010 (Epub)
24. Pal SK, Mortimer J (2009) Triple-negative breast cancer: novel therapies and new directions. Maturitas 63:269–274
25. Corkery B, Crown J, Clynes M et al (2009) Epidermal growth factor receptor as a potential therapeutic target in triple-negative breast cancer. Ann Oncol 20:862–867
26. Inbar-Rozensal D, Castiel A, Visochek L et al (2009) A selective eradication of human nonhereditary breast cancer cells by phenanthridine-derived polyADP-ribose polymerase inhibitors. Breast Cancer res 11:R78

Research Article

Reduced Plasma Level of CXC Chemokine Ligand 7 in Patients with Pancreatic Cancer

Junichi Matsubara[1,2], Kazufumi Honda[1], Masaya Ono[1], Yoshinori Tanaka[3], Michimoto Kobayashi[3], Giman Jung[3], Koji Yanagisawa[4], Tomohiro Sakuma[4], Shoji Nakamori[5], Naohiro Sata[6], Hideo Nagai[6], Tatsuya Ioka[7], Takuji Okusaka[8], Tomoo Kosuge[8], Akihiko Tsuchida[9], Masashi Shimahara[10], Yohichi Yasunami[11], Tsutomu Chiba[2], Setsuo Hirohashi[1], and Tesshi Yamada[1]

Abstract

Background: Early detection is essential to improve the outcome of patients with pancreatic cancer. A noninvasive and cost-effective diagnostic test using plasma/serum biomarkers would facilitate the detection of pancreatic cancer at the early stage.

Methods: Using a novel combination of hollow fiber membrane–based low-molecular-weight protein enrichment and LC-MS-based quantitative shotgun proteomics, we compared the plasma proteome between 24 patients with pancreatic cancer and 21 healthy controls (training cohort). An identified biomarker candidate was then subjected to a large blinded independent validation ($n = 237$, validation cohort) using a high-density reverse-phase protein microarray.

Results: Among a total of 53,009 MS peaks, we identified a peptide derived from CXC chemokine ligand 7 (CXCL7) that was significantly reduced in pancreatic cancer patients, showing an area under curve (AUC) value of 0.84 and a P value of 0.00005 (Mann–Whitney U test). Reduction of the CXCL7 protein was consistently observed in pancreatic cancer patients including those with stage I and II disease in the validation cohort ($P < 0.0001$). The plasma level of CXCL7 was independent from that of CA19-9 (Pearson's $r = 0.289$), and combination with CXCL7 significantly improved the AUC value of CA19-9 to 0.961 ($P = 0.002$).

Conclusions: We identified a significant decrease of the plasma CXCL7 level in patients with pancreatic cancer, and combination of CA19-9 with CXCL7 improved the discriminatory power of the former for pancreatic cancer.

Impact: The present findings may provide a new diagnostic option for pancreatic cancer and facilitate early detection of the disease. *Cancer Epidemiol Biomarkers Prev; 20(1); 160–71. ©2011 AACR.*

Authors' Affiliations: [1]Chemotherapy Division, National Cancer Center Research Institute, Tokyo; [2]Department of Gastroenterology and Hepatology, Kyoto University Graduate School of Medicine, Kyoto; [3]New Frontiers Research Laboratories, Toray Industries, Kamakura; [4]BioBusiness Group, Mitsui Knowledge Industry, Tokyo; [5]Department of Surgery, Osaka National Hospital, National Hospital Organization, Osaka; [6]Department of Surgery, Jichi Medical University, Shimotsuke; [7]Department of Hepatobiliary and Pancreatic Oncology, Osaka Medical Center for Cancer and Cardiovascular Diseases, Osaka; [8]Hepatobiliary and Pancreatic Oncology and Hepatobiliary and Pancreatic Surgery Divisions, National Cancer Center Hospital, Tokyo; [9]Third Department of Surgery, Tokyo Medical University, Tokyo; [10]Department of Oral Surgery, Osaka Medical College, Osaka; and [11]Department of Regenerative Medicine and Transplantation, Fukuoka University Faculty of Medicine, Fukuoka, Japan

Introduction

Pancreatic adenocarcinoma is one of the most aggressive and lethal of diseases. The overall 5-year survival rate of patients with pancreatic cancer is less than 5%, which is the lowest among the more common cancers (1, 2), and the disease is the fifth leading cause of cancer death in Japan and the fourth in the United States, with greater than 23,000 estimated annual deaths in Japan and greater than 33,000 in the United States (3, 4). The 5-year survival rate of patients who were able to undergo surgical resection reaches 20% to 40% (5, 6), but the majority of pancreatic cancer patients have already developed lymph node and/or distant organ metastasis at their first clinical presentation, and only about 20% of patients are able to undergo radical resection (7, 8). The introduction of gemcitabine has significantly improved the overall survival of patients with unresectable pancreatic cancer, but their median survival period still remains about 6 months (9–11). These statistics

demonstrate that early detection is essential for improving the outcome of patients with pancreatic cancer.

Computed tomography (CT), magnetic resonance imaging (MRI), and positron emission tomography (PET) are not cost-effective for the screening of pancreatic cancer because of the relatively low incidence of the disease. If a noninvasive and cost-effective screening test employing plasma/serum markers could be devised, it would significantly facilitate the early detection of pancreatic cancer. However, no biomarker suitable for screening of pancreatic cancer is currently available (12). CA19-9 is an established biomarker useful for the follow-up of pancreatic cancer patients receiving treatment, but has not been recommended for cancer screening because of its insufficient sensitivity and specificity (7, 13). Therefore, the discovery of a new biomarker that would be able to supplement CA19-9 has been anticipated.

Recently, advanced proteomic technologies based on mass spectrometry (MS) have been increasingly applied to studies of clinical samples to identify new biomarkers of various diseases (14) including pancreatic cancer (12, 15). It is anticipated that alterations in the protein content of clinical samples reflect the biological status of patients more directly than those in mRNA (16). We previously developed a new shotgun proteome platform, 2-Dimensional Image Converted Analysis of Liquid chromatography and mass spectrometry (2DICAL; ref. 17). 2DICAL is highly advantageous for clinical proteomics because of its high quantification accuracy and throughput. Using 2DICAL, we have been able to identify several plasma/serum biomarkers useful for cancer detection and therapy tailoring (18–20).

The serum/plasma proteome accumulates a large variety of disease-related alterations and is considered to be a rich source of biomarkers. However, for proteomic analysis of blood samples, the efficient depletion of a handful of particularly abundant proteins, such as albumin and immunoglobulin, has been challenging (21). Recently, we developed a novel method for the pretreatment of serum/plasma using the high-performance hollow fiber membrane (HFM) filtration technique (22). This method employs multistage filtration and cascaded cross-flow processes, enabling fully automated separation of proteins below a predetermined molecular weight (22). As the more abundant plasma proteins generally have relatively large molecular weights, they can be efficiently eliminated using the HFM technique.

To identify new biomarkers that might be useful for the early detection of patients with pancreatic cancer, we performed a comprehensive analysis of low-molecular-weight (LMW) plasma proteins in these patients using a combination of the HFM and 2DICAL techniques. A large variety of LMW proteins are known to be secreted from diseased tissues and can serve as good diagnostic biomarkers for various diseases (23, 24). Here, we report the identification and validation of an LMW chemotactic cytokine, CXC chemokine ligand 7 (CXCL7), as a novel biomarker for pancreatic cancer.

Patients and Methods

Plasma samples

Plasma samples were collected prospectively from 282 individuals (K. Honda, T. Okusaka, K. Felix, S. Nakamori, N. Sata, H. Nagai, et al., manuscript submitted) including healthy volunteers and newcomers to mainly departments of gastroenterology between August 2006 and October 2008 at the following 7 hospitals in Japan: National Cancer Center Hospital (NCCH), Osaka National Hospital (ONH), Jichi Medical School Hospital, Osaka Medical College (OMC), Tokyo Medical University Hospital (TMUH), Osaka Medical Center for Cancer and Cardiovascular Diseases, and Fukuoka University Hospital. This multi-institutional collaborative study group was organized by the "Third-Term Comprehensive Control Research for Cancer" conducted by the Ministry of Health, Labour and Welfare of Japan, and as part of the International Cancer Biomarker Consortium (25). The procedures used for collection and storage were kept uniform for all plasma samples.

The 282 plasma samples were split into 2 study sets (referred to as the training and validation cohorts). The training cohort comprised 45 individuals including patients with untreated pancreatic cancer at NCCH ($n = 19$) and TMUH ($n = 5$), and healthy controls at NCCH ($n = 2$), TMUH ($n = 9$), OMC ($n = 6$), and ONH ($n = 4$). The validation cohort comprised 237 individuals including 140 patients with pancreatic cancer, 10 patients with chronic pancreatitis, and 87 healthy controls. All patients diagnosed as having pancreatic cancer had histologically or cytologically proven ductal adenocarcinoma. Demographic and laboratory data are summarized in Table 1. The staging of pancreatic cancer was in accordance with the TNM classification of the International Union against Cancer (UICC).

Blood was collected in a tube with EDTA at the time of diagnosis. The plasma was separated by centrifugation and frozen at −80°C until analysis. Samples showing macroscopic evidence of hemolysis were excluded from the current analysis. Written informed consent was obtained from every subject before blood collection. The protocol of this study was reviewed and approved by the institutional ethics committee boards of each participating institution.

Depletion of high-molecular-weight plasma proteins

The plasma samples of the training cohort were filtered through a 0.22-μm pore size filter. Five hundred microliters of the sample was diluted by adding 3.5 mL of 25 mmol/L of ammonium bicarbonate buffer (pH 8.0). The total 4 mL of the diluted plasma was processed as previously described (22). After 1 hour of fully automated operation, LMW proteins with molecular weights smaller than 60 kDa were recovered (Supplementary Fig. S1) and lyophilized.

The concentration of β2-microglobulin before and after HFM treatment was measured using an ELISA kit (Human Beta-2 Microglobulin ELISA Kit: Alpha Diagnostic Intl. Inc.) to ensure consistent recovery.

Table 1. Clinicopathologic characteristics of individuals in training and validation cohorts

	Training cohort (n = 45)			Validation cohort (n = 237)				
	Healthy control	Cancer	P	Healthy control	Cancer	P^f	Chronic pancreatitis	P^f
No. of patients	21	24		87	140		10	
Sex, n			0.205^a			0.485^a		0.487^a
Male	17	15		56	83		8	
Female	4	9		31	57		2	
Age, y			<0.001			<0.001		0
mean (SD)	40 (13)	64 (7)	NA	43 (16)	66 (10)	NA	58 (13)	NA
Tumor location			NA			NA		NA
Head	—	14		—	59		—	
Body or tail	—	10		—	76		—	
Unknown	—	0		—	5		—	
Clinical stage			NA			NA		NA
I	—	1		—	5		—	
II	—	6		—	25		—	
III	—	4		—	40		—	
IV	—	13		—	70		—	
CA19-9 median, U/mL	5.5	1,109	<0.001	10.2	476	<0.001	5.2	0.06
>37.0 (ULN), no. of patients	2	19		4	110		0	
DUPAN-2 median, U/mL	12	540	<0.001	12	375	<0.001	25	<0.001
>150.0 (ULN), no. of patients	1	19		0	92		1	
CEA median, ng/mL	1.7	6.0	<0.001	1.7	3.5	<0.001	2.6	0.110
>5.0 (ULN), no. of patients	1	12		5	49		1	
Total bilirubin median, mg/dL	0.5	0.4	0.688	0.5	0.5	0.574	0.5	0.4
>1.2 (ULN), no. of patients	0	2		4	18		0	
CXCL7								
Mass spectrometry peak intensity[b], mean (SD)	332 (240)	138 (346)	$<0.001^d$	—				
Protein intensity[c], mean (SD)	4.14 (0.18)	3.83 (0.28)	$<0.001^e$	4.18 (0.14)	3.92 (0.28)	$<0.001^e$	3.99 (0.10)	$<0.001^e$

NOTE. Wilcoxon test was applied to assess differences in values.

Abbreviations: CEA, carcinoembryonic antigen; NA, not applicable; ULN, upper limit of normal.

[a]Calculated by Fisher's exact test.

[b]Intensity of the corresponding peak measured by quantitative mass spectrometry.

[c]Measured using reverse-phase protein microarrays (logarithmic variable).

[d]Calculated by Mann–Whitney U-test.

[e]Calculated by Welch's t test.

[f]Compared with healthy controls.

Liquid chromatography/mass spectrometry

The HFM-treated samples were digested with sequencing grade-modified trypsin (Promega) and analyzed in duplicate using a nano-flow high-performance liquid chromatography (HPLC; NanoFrontier nLC, Hitachi High-technologies) connected to an electrospray ionization quadrupole time-of-flight (ESI-Q-TOF) mass spectrometer (Q-Tof Ultima, Waters).

MS peaks were detected, normalized, and quantified using the in-house 2DICAL software package, as described previously (17). A serial identification (ID) number was applied to each of the MS peaks detected (1 to 53,009). The stability of LC-MS was monitored by calculating the correlation coefficient (CC) and coefficient of variance (CV) of every measurement. The mean CC ± SD and CV ± SD for all 53,009 peaks observed in the 45 duplicate runs were as high as 0.946 ± 0.042 and as low as 0.053 ± 0.010, respectively.

Protein identification by tandem MS (MS/MS)

Peak lists were generated using the Mass Navigator software package (version 1.2; Mitsui Knowledge Industry) and searched against the SwissProt database (downloaded on April 22, 2009) using the Mascot software package (version 2.2.1; Matrix Science). The search parameters used were as follows. A database of human proteins was selected. Trypsin was designated as the enzyme, and up to 1 missed cleavage was allowed. Mass tolerances for precursor and fragment ions were ± 0.6 Da and ± 0.2 Da, respectively. The score threshold was set to $P < 0.05$ based on the size of the database used in the search. If a peptide was matched to multiple proteins, the protein name with the highest Mascot score was selected.

Western blot analysis

Primary antibodies used were a rabbit polyclonal antibody against platelet basic protein (PBP) precursor (Sigma) and a mouse monoclonal antibody against human complement C3b-α (PROGEN). The anti-PBP antibody recognizes all the known cleaved forms of PBP including CTAP-III and NAP-2. Six microliters of 1:10 diluted plasma sample was separated by SDS-PAGE and electroblotted onto a polyvinylidene difluoride (PVDF) membrane. The membrane was then incubated with the primary antibody and subsequently with the relevant horseradish peroxidase (HRP)-conjugated anti-rabbit or anti-mouse IgG, as described previously (26, 27). Blots were developed using an enhanced chemiluminescence (ECL) detection system (GE Healthcare).

Reverse-phase protein microarray

The plasma samples were passed through IgY microbeads (Seppro-IgY12, Sigma-Aldrich) using an automated Magtration System SA-1 (Precision System Science) in accordance with the manufacturer's instructions to reduce the 12 most abundant plasma proteins. The flow-through portion was serially diluted 1:50, 1:100, 1:200, and 1:400 using a Biomek 2000 Laboratory Automation Robot (Beckman Coulter) and randomly plotted onto ProteoChip glass slides (Proteogen) in quadruplicate in a 6,144-spot/slide format using a Protein Microarrayer Robot (Kaken Geneqs). The spotted slides were incubated overnight with the anti-PBP precursor antibody and then with biotinylated anti-rabbit IgG (Vector Laboratories) and subsequently with streptavidin-HRP conjugate (GE Healthcare). The peroxidase activity was detected using the Tyramide Signal Amplification (TSA) Cyanine 5 System (PerkinElmer). The slides were counterstained with Alexa Fluor 546-labeled goat anti-human IgG (Invitrogen; spotting control).

The stained slides were scanned on a microarray scanner (InnoScan 700AL; Innopsys). Fluorescence intensity, determined as the mean value of quadruplicate samples, was determined using the Mapix software package (Innopsys). All determined intensity values were transformed into logarithmic variables.

The reproducibility of the reverse-phase protein microarray assay was determined by repeating the same experiment, as reported previously (28). A plasma sample after reduction of the 12 most abundant plasma proteins was serially diluted within a range of 25- to 6,400-fold. Each diluted sample was spotted in quadruplicate onto glass slides and blotted with the anti-PBP antibody. In a representative quality control experiment, the CC value was 0.980 between days and the median CV was 0.047 among the quadruplicates.

Multiplex assay

The levels of CXCL7 in plasma samples were measured using a Milliplex Human Cytokine/Chemokine panel III kit (Millipore) in accordance with the manufacturer's instructions.

Statistical analysis

Statistical significance of intergroup differences was assessed with the Wilcoxon test, Mann–Whitney U test, Welch's t test, or Fisher's exact test, as appropriate. The area under the curve (AUC) of the receiver-operating characteristic (ROC) was calculated for each marker to evaluate its diagnostic significance. A composite index of 2 markers was generated using the results of multivariate logistic regression analysis, which also enabled the calculation of sensitivity, specificity, and the ROC curve. Statistical analyses were performed using an open-source statistical language R (version 2.7.0) with the optional module Design package.

Results

Plasma proteins associated with pancreatic cancer

A plasma sample from 1 healthy volunteer was processed 3 times using the HFM filtration technique. The concentration of β2-microglobulin before and after HFM treatment was measured. The recovery rates were